Japanese Journal of Radiology (2019) 37:354–370
https://doi.org/10.1007/s11604-019-00832-4

INVITED REVIEW

Imaging of extracranial head and neck lesions in cancer patients: a symptom-based approach

Takashi Hiyama[1] · Kotaro Sekiya[1] · Hirofumi Kuno[1] · Shioto Oda[1] · Masahiko Kusumoto[1,2] · Manabu Minami[3] · Tatsushi Kobayashi[1]

Received: 28 January 2019 / Accepted: 17 March 2019 / Published online: 25 March 2019

Abstract

Besides intracranial lesions, neurological symptoms are also caused in cancer patients by extracranial lesions in the head and neck. Common symptoms caused by such lesions include visual loss, visual field defect, diplopia, ptosis, sensory abnormalities of the head and neck region, facial nerve palsy, dysphagia, dysarthria, hoarseness, and syncope. Some cancer patients often have multiple cranial nerve involvement, which is associated with several syndromes such as jugular foramen syndrome. The main causes of cranial nerve dysfunction due to extracranial lesions include bone and nodal metastasis, perineural tumor spread, inflammation, and radiation injury. The location of the lesions causing the neurological symptom may be estimated by the symptoms and physical examination. However, CT/MRI is critical for reaching the final diagnosis and for treatment planning and management of the cancer patients. Moreover, early identification of the extracranial lesions may significantly affect patient care and alter outcomes. Thus, radiologists should be familiar with imaging findings of the common neurological disorders and the complex anatomy of the head and neck region, which should be checked in cancer patients with neurological symptoms.

Keywords Cranial nerve · Cancer · Head and neck · CT · MRI

Introduction

Malignant neoplasms are the most common cause of death, and 1369 per 100,000 people are diagnosed as new cancer patients each year in Japan [1]. Cancer patients present various symptoms, including cranial nerve (CN) symptoms that occur in 15–46% of cancer patients [2–4].

In the clinical setting, physicians are able to deduce the probable causes of symptoms and location of the pathologies based on neurological and physical findings. CT and MRI are useful in confirming the lesions and reaching the final diagnosis. Although CN symptoms are caused by intracranial lesions such as brain metastasis and meningeal dissemination, the extracranial lesions such as skull base metastasis and head and neck lesions also cause cranial nerve symptoms. Therefore, radiologists need to be familiar with these anatomical structures and corresponding imaging findings and to assess them in cancer patients with neurological symptoms. However, there are few imaging review articles about the extracranial lesions with cranial nerve involvement from the viewpoint of symptoms. In the following sections, we discuss the anatomy of the skull base and head and neck that is related to cranial neurological symptoms and describe the major pathologies in cancer patients from a neurological point of view. Anatomical checkpoints and major causes that affect CNs are discussed in Table 1.

This article was presented in part at the 103rd annual meeting of the Radiological Society of North America (RSNA) in Chicago, 2017. It received a Certification of Merit for educational exhibit.

✉ Takashi Hiyama
med-tak@hotmail.com

[1] Department of Diagnostic Radiology, National Cancer Center Hospital East, 6-5-1, Kashiwanoha, Kashiwa, Chiba 277-8577, Japan

[2] Department of Diagnostic Radiology, National Cancer Center Hospital, 5-1-1, Tsukiji, Chuo-ku, Tokyo 104-0045, Japan

[3] Department of Diagnostic and Interventional Radiology, Faculty of Medicine, University of Tsukuba, 2-1-1 Amakubo, Tsukuba, Ibaraki 305-8576, Japan

Table 1 Summary of cranial nerve symptoms, associated nerves, checkpoints, and causes

Symptom	Nerves	Checkpoints	Causes
Visual loss and visual field defect	II	Globe Optic nerve Orbital apex	Choroidal metastasis Optic neuritis/perineuritis Optic nerve metastasis Orbital metastasis Sinusitis/mucocele
Diplopia	III, IV, VI	Extraocular muscles Superior orbital fissure Cavernous sinus Dorello canal Petrous apex	Orbital metastasis Perineural spread Sinusitis/mucocele Skull base metastasis Osteomyelitis
Ptosis	III Sympathetic nerve	Eyelid Extraocular muscles Meckel cave Carotid sheath Mediastinum	Mechanical ptosis Neurogenic ptosis Myogenic ptosis
Trigeminal neuralgia	V	Mandible Masticator space Pterygopalatine fossa Inferior orbital canal Foramen rotundum Foramen ovale Meckel cave	Metastasis Medication-related osteonecrosis of the jaw Perineural spread Skull base osteomyelitis
Otalgia	V3, VII, IX, X, C2, C3	Ear, oral cavity, Pharynx, Supraglottic larynx	Head and neck cancer Recurrence
Dysgeusia	V3 Chorda tympani	Submandibular space Masticator space Temporal bone	Perineural spread Metastasis
Facial nerve paralysis	VII	Parotid gland Temporal bone	Parotid cancer Perineural spread Metastasis Petrositis
Dysphagia Dysarthria	IX, X, XII	Oral cavity Pharynx, Larynx Carotid sheath Jugular foramen	Perineural spread Skull base osteomyelitis Metastasis
Hoarseness	X Recurrent laryngeal nerve	Mediastinum TEG Larynx Carotid sheath Cavernous sinus Jugular foramen	Lung cancer Thyroid cancer Nodal metastasis Skull base osteomyelitis Skull base metastasis Iatrogenic injury
Syncope	IX, X	Carotid sinus Carotid sheath	Nodal metastasis Perineural spread

II optic nerve, *III* oculomotor nerve, *IV* trochlear nerve, *V* trigeminal nerve, *VI* abducens nerve, *VII* facial nerve, *VIII* vestibulocochlear nerve, *X* vagus nerve, *XI* accessory nerve, *XII* hypoglossal nerve, *C* cervical spinal nerve, *TEG* tracheoesophageal groove

Visual loss and visual field defect

Associated anatomy

Visual loss or visual field defect may be caused by any lesion in the ocular globe or visual pathway. The ocular globe contains the lens and vitreous body and is layered by the retina, choroid, and sclera (Fig. 1a, b) [5]. The optic pathway comprises the optic nerve, chiasm, and optic tract. The optic nerve is derived from the mesencephalon, covered with meninges, and has subarachnoid space (Fig. 1c). The optic canal is located at orbital apex and close to the anterior crinoid process and sphenoid sinus or Onodi cell, which is the posterior extension of the ethmoid sinus. Patterns of visual field defects differ depending on the location of lesions. For example, unilateral extracranial lesions such as choroidal metastasis or radiation-induced optic neuropathy cause ipsilateral visual disturbance. Thus, the ocular globe and optic nerve should be assessed for

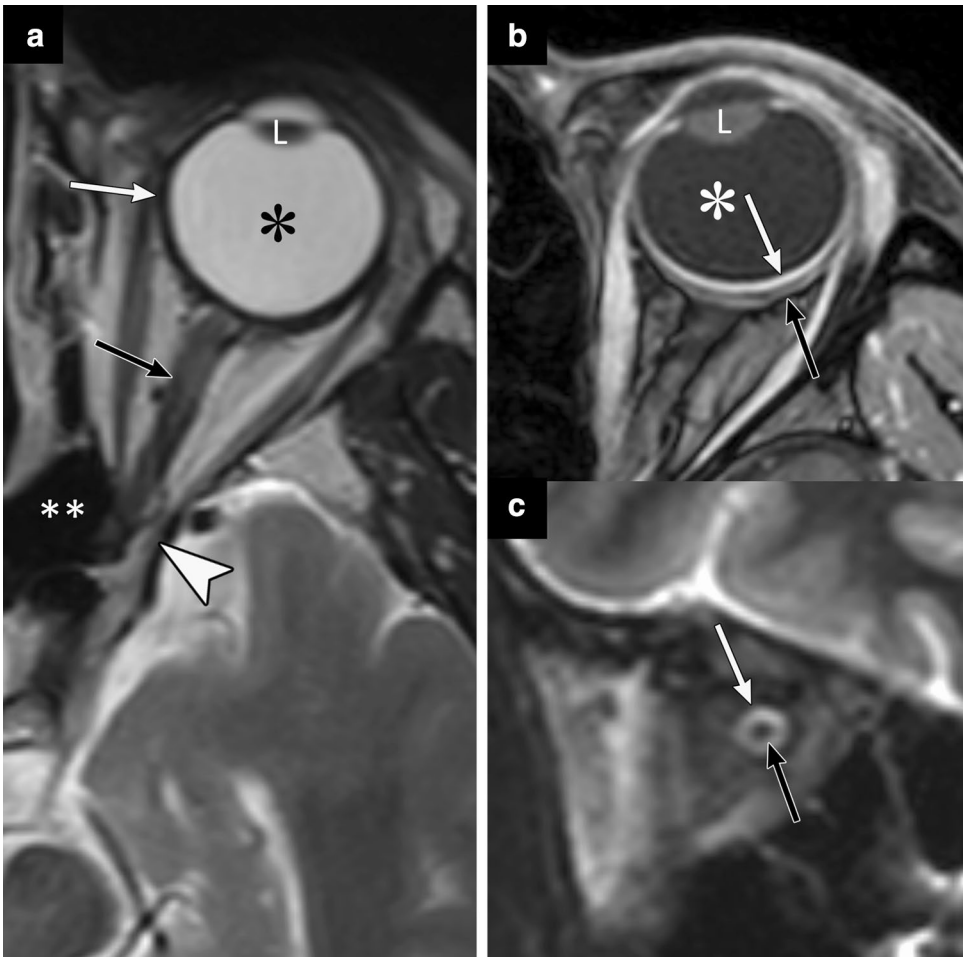

Fig. 1 Anatomy of the orbit. **a** T2-weighted MR image showing the ocular globe (white arrow), optic nerve (black arrow), and orbital apex (white arrowhead). **b** Post-contrast T1-weighted MR image showing the retina and choroid as the inner layer (white arrow) and the sclera as the outer layer (black arrow). **c** Coronal STIR (short tau inversion recovery) image showing the optic sheath (white arrow) and optic nerve (black arrow). *L* lens, *asterisk* vitreous body, *double asterisk* sphenoid sinus

patients with visual disorders besides intracranial visual pathway.

Pathology

Choroidal metastasis

Choroidal metastasis accounts for about 60% of metastasis in the orbital fossa [6]. It is likely to occur in the choroidal membrane, because the choroid is well vascularized. The metastatic site is 80% proximal to the equator, 12% near the macula, and 8% distal from the equator [7]. Breast and lung cancer is the cause in more than half of the patients with choroidal metastasis [7]. Other primary tumors include gastrointestinal, skin, and urinary cancer [8].

Choroidal metastasis often shows a flat or lenticular morphology (Fig. 2a). On MRI, these lesions show mild hyperintensities on T1-weighted MR images, while they show hypointensities on T2-weighted MR images when compared with the vitreous body; however, about 20% of metastatic lesions show hyperintensities on T1-weighted MR images [9]. When exudative retinal detachment also occurs, it is visible as liquid retention under the retina, and, in many cases, shows high attenuation on CT images and hyperintensities on T1-weighted MR images. Multiple choroidal and contralateral ocular globe lesions, as well as brain and bone metastasis, indicate choroidal metastasis. Besides choroidal metastasis, radiation-induced cataracts and retinopathy may also cause visual impairment, but it is difficult to identify these lesions by CT/MRI.

Radiation-induced optic neuritis and perineuritis

Radiation-induced optic neuritis develops as unilateral or bilateral progressive visual loss about 6–24 months after radiotherapy [10]. At fraction sizes < 2 Gy, severe optic neuropathy after cranial radiotherapy is unusual with doses less than 55 Gy, but increases to 3–7% with doses of 55–60 Gy, and to 7–20% for doses > 60 Gy [11]. On MRI, high signal intensities are observed in the optic nerve on T2-weighted MR and STIR images, and contrast enhancement is seen in the acute phase. Enhancement of the optic nerve and chiasm on T1-weighted MR images may resolve in several months, and the atrophy of the optic nerve may progress [12, 13]. In

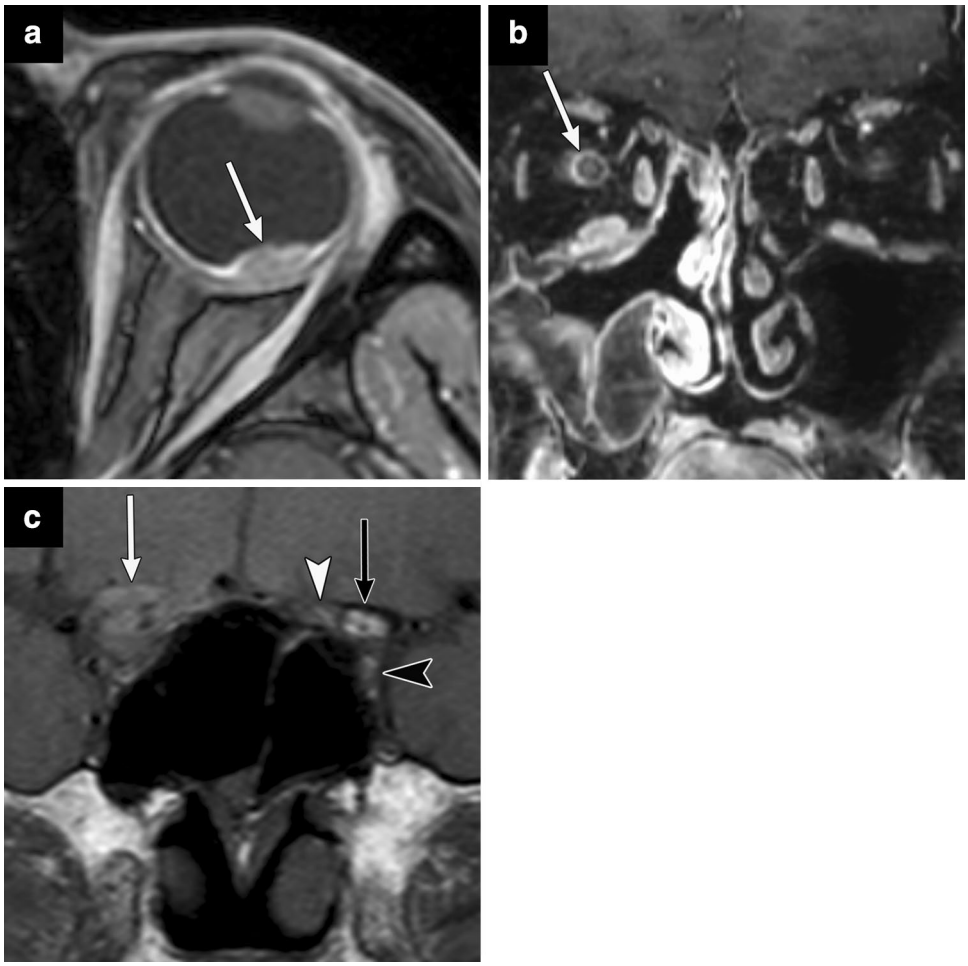

Fig. 2 Three cases of visual impairment. **a** A 20-year-old woman with choroidal metastasis and visual defect on the left eye. Post-contrast T1-weighted MR image showing flat-shaped metastasis to the choroidal membrane. **b** A 40-year-old male with right progressive vision loss after radiotherapy for nasopharyngeal cancer. Post-contrast T1-weighted MR image shows peripheral enhancement of the optic nerve (white arrow). He was diagnosed with radiation-induced optic perineuritis. **c** A 70-year-old male with prostate cancer and right progressive visual loss and diplopia. T1-weighted MR image shows metastasis to the right clinoid process involving the optic canal and superior orbital fissure (white arrow). The normal left anterior clinoid process (black arrow), optic canal (white arrowhead), and superior orbital fissure (black arrowhead) are shown

optic perineuritis, circumferential enhancement of the optic nerve sheath is shown (Fig. 2b).

Optic nerve metastasis

Carcinomas may metastasize directly to the optic nerve or optic nerve sheath or via the subarachnoid space around the optic nerve sheath by meningeal dissemination. Past reports on optic nerve metastasis did not strictly distinguish these entities. One study reported on three cases (1.3%) showing metastasis to the optic nerve in a total of 227 patients with orbital metastasis [6].

Metastatic carcinomas to the optic nerve show iso- or moderate hyperintensities on T1-weighted MR images and hypointensities on T2-weighed images, and their enhancement is homogeneous. When the tumor invades, mainly in the subarachnoid space around the optic nerve, MRI findings are similar to those of optic nerve sheath meningioma [14]. However, optic nerve sheath meningioma show calcification on CT and slower growth compared to optic nerve metastasis.

Orbital metastasis

Herein, we discuss metastasis to the orbital fat and bone, excluding the eye ball, optic nerve and sheath, and extraocular muscles. Orbital metastasis accounts for 1–13% of orbital tumors and is found in 2–3% of patients with cancer [15]. Breast cancer is the most common primary tumor leading to orbital metastasis, followed by lung cancer, prostate cancer, and melanoma. However, in children, neuroblastoma accounts for 89% of cases as the primary tumor [16].

Orbital metastasis shows low signal intensities on T1-weighted MR images and moderately high signal intensities on T2-weighted MR images. Bone metastasis of the orbit, especially that to the sphenoid triangle and anterior clinoid process, tends to compress the optic nerve, leading to visual impairment (Fig. 2c) [17, 18].

Sinusitis, mucocele

Sinusitis or mucocele, especially in the sphenoid sinus, can cause visual impairment due to inflammation or compression of the optic nerve [19]. Radiographic evidence

of chronic rhinosinusitis has been reported in up to 73% of patients with nasopharyngeal carcinoma after treatment with combined chemotherapy and radiotherapy [20], although the majority of these patients are treated with medical therapy alone. Mucocele also occurs after radiotherapy due to ostial obstruction by mucosal swelling [21]. MR signal intensity of the mucocele is variable depending on the content. Hypointensities on T1-weighted and signal void on T2-weighted MR images reflect inspissated mucin, while hyperintensities on T1- and T2-weighted MR images reflect hydrated secretion and high protein content [22].

Diplopia

Associated anatomy

Diplopia may be caused by disorders of the oculomotor (CN III), trochlear (CN IV), and abduction (CN VI) nerves, as well as by extraocular muscular disorders. CN III, IV, and VI run in the cistern in front of the brainstem and enter the cavernous sinus (Fig. 3). CN III, IV, and the first and second branch of the trigeminal nerve (V1 and V2) pass within the lateral wall of the cavernous sinus. On the other hand, CN VI passes inside of the cavernous sinus [23]. Then, CN III, IV, V1, and VI enter the orbit via the superior orbital fissure. The involvement of these nerves at the superior orbital fissure causes superior orbital fissure syndrome, and involvement of the optic canal in addition to the superior orbital fissure causes the orbital apex syndrome [24, 25]. The sympathetic nerve joins the under surface of CN VI in the cavernous sinus shortly before fusing with the V1 to enter the orbit [26]. CN VI passes the Dorello canal, located at the petrous apex, and under the petroclinoid ligament [27]. The Meckel cave containing the Gasser ganglion is embedded in the trigeminal impression at the anterior surface of the petrous apex.

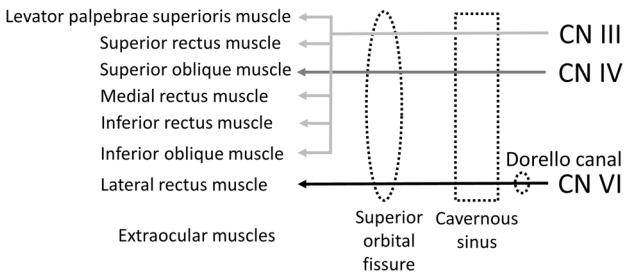

Fig. 3 Anatomy of CN III, IV and VI. These nerves run through the cavernous sinus and superior orbital fissure, and innervate the extraocular muscles. CN VI passes the Dorello canal before entering the cavernous sinus

Pathology

Extraocular muscle metastasis

Among types of orbital metastasis, metastasis to the extraocular muscle is estimated to represent 5% of cases [28]. Two-thirds of the cases of extraocular muscle metastasis are unilateral, and the remaining one-third involves bilateral metastasis [29]. A third of patients show multiple extraocular muscle metastases [29]. Malignant melanoma, breast cancer, and carcinoid are common as the primary tumor, and the lateral rectus muscle is the most common site of metastasis. Diplopia and eyelid ptosis are presented as symptoms. CT and MRI demonstrate nodular mass with sharp margins, which often spare relatively hypovascular tendons [29, 30] (Fig. 4a). Enophthalmos may be observed in patients with scirrhous breast cancer or gastrointestinal carcinoma secondary to fibrotic contraction of the orbital fat, resulting in posterior globe retraction and restriction of eye movements [15, 31].

Lesions of the cavernous sinus

Lesions involving the cavernous sinus in cancer patients include metastasis, perineural spread (PNS) from head and neck cancer (Fig. 4b), and sinusitis-induced inflammation after radiotherapy. These lesions cause diplopia due to involving the ocular motor nerves. Clinical symptoms typically consist of various combinations of ocular motor nerve impairments (CN III, VI, IV), Horner syndrome (sympathetic nerve), and sensory loss of CN V1 and V2. Cavernous sinus syndrome is characterized by these cranial neuropathies [32].

Pseudo-Gradenigo syndrome

Petrous apex lesions may involve CN V and VI, and cause abducens nerve paralysis (Fig. 4c). Gradenigo syndrome refers to a triad of otorrhea, diplopia due to CN VI involvement, and facial pain due to CN V involvement, which is caused by inflammation due to otitis media spreading to the petrous apex [33]. However, malignant tumors such as nasopharyngeal carcinoma may mimic Gradenigo syndrome, as they may invade the petrous apex and obstruct the Eustachian tube at the same time, resulting in otitis media. In some reports, this entity is referred to as the pseudo-Gradenigo syndrome [34].

Ptosis

Associated anatomy

The tarsal plates are found in the upper eyelid, and contribute to its shape and support. The levator palpebrae superioris

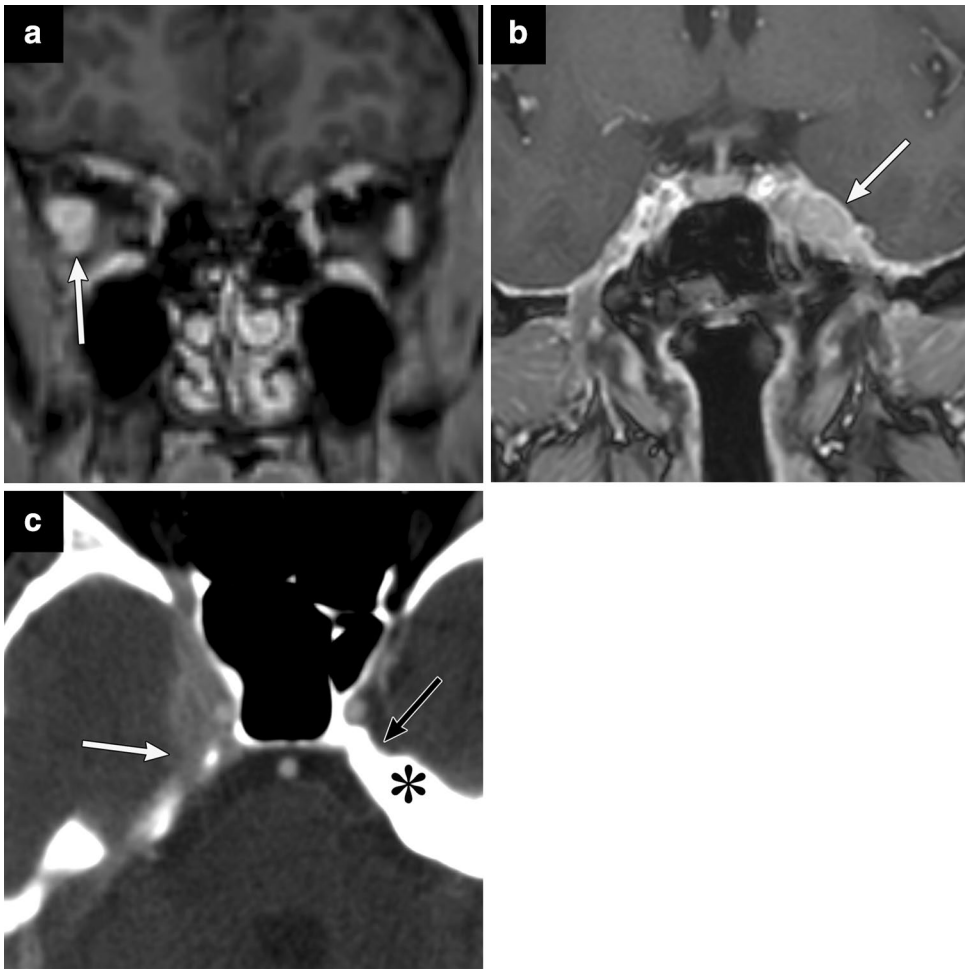

Fig. 4 Three cases of diplopia. **a** A 30-year-old female with breast cancer, presenting with diplopia and right abducent paralysis. Post-contrast T1-weighted MR image shows metastasis to the right lateral rectus muscle (white arrow). **b** A 50-year-old female with parotid cancer who had diplopia and left ptosis. Post-contrast T1-weighted MR image shows perineural spread along the V3 extending to the Meckel cave and cavernous sinus (white arrow). **c** A 40-year-old female with breast cancer who presented right abducent paralysis and facial numbness. The tumor extends to the petrous apex and involves CN VI and V (white arrow) on contrast-enhanced CT image. The normal left petrous apex (asterisk) and trigeminal impression (black arrow) are shown

muscle, innervated by CN III, and Muller muscle, innervated by the sympathetic nervous system, attach to the tarsal plate and rise up the upper eyelid. The sympathetic nervous system also innervates the pupillary dilator muscles, and its malfunction causes miosis in addition to ptosis. The sympathetic nerve arises from C8 to T2, travels along the paravertebral body and carotid sheath, and enters the carotid canal [35]. A triad of ipsilateral ptosis, pupillary miosis, and facial anhidrosis constitutes Horner syndrome.

Pathology

Ptosis is classified as mechanical, neurogenic, or myogenic based on the etiology.

Mechanical ptosis

Mechanical ptosis is caused by edema or tumors of the upper eyelid. Among patients with cancer, mechanical ptosis is caused by metastasis to eyelids or extraocular muscles, affecting patients between 50 and 80 years of age [36]. Up to 50% of the cases arise from breast carcinoma (Fig. 5a) [37], but other primary sites have been reported as origins, including the lung, stomach, esophagus, and kidney. Eyelid metastasis is usually unilateral and is classified morphologically into nodular, infiltrative, or ulcerated, with infiltrative metastasis being common in patients with breast cancer [37].

Neurogenic ptosis

Neurogenic ptosis is caused by disturbance of CN III or the sympathetic nerve. CN III may be involved due to orbital or cavernous sinus lesions, while sympathetic nerve disturbances could occur anywhere along the nerve [35]. Pancoast tumor and mesothelioma at the apex of the lung, thyroid tumor, and tumors at the base of the skull may also involve sympathetic nerves [38] (Fig. 5b). Thus, a thorough examination of the sympathetic nerve should be performed in a patient with neurogenic ptosis.

Myogenic ptosis

One of the causes of myogenic ptosis is due to anti-acetylcholine receptor antibody [39]. Although thymoma is known

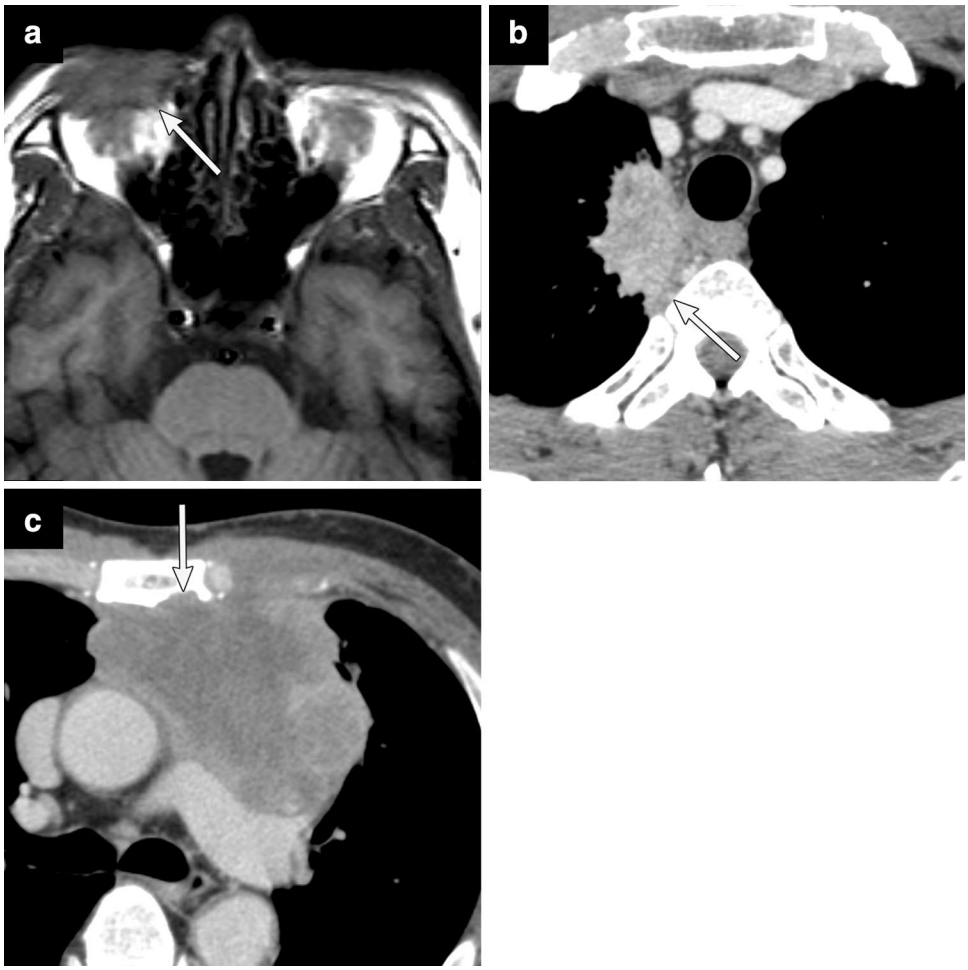

Fig. 5 Three cases of ptosis. **a** A 58-year-old female with breast cancer and right ptosis. T1-weighted MR image shows metastasis to the right eyelid (white arrow). **b** A 44-year-old male with lung cancer and Horner syndrome. Contrast-enhanced CT image shows the lung cancer invading to the paravertebral area. Involvement of the sympathetic nerve is highly suspected (white arrow indicating the usual position of the right sympathetic nerve). **c** A 61-year-old male with thymic carcinoma and bilateral ptosis. Contrast-enhanced CT image shows an anterior mediastinal mass with invasion of the sternum

as a tumor associated with myogenic ptosis, thymic cancer is also reported (Fig. 5c) [40]. Lambert–Eaton myasthenic syndrome (LEMS) constitutes an autoimmune disorder of the neuromuscular junctions causing myogenic ptosis. Lung cancer, especially small cell carcinoma, may be associated with antibodies against voltage-gated calcium channel (VGCC), the binding of which to VGCC leads to neuromuscular transmission disturbances. Several cases of LEMS associated with prostate carcinoma, lymphoma, and leukemia were previously reported [41].

Trigeminal neuralgia

Associated anatomy

The trigeminal nerve innervates most areas of the face and is involved in sensation. It exits the brainstem and branches into the V1, V2, and mandibular nerve (V3) in the Meckel cave [42]. V1 and V2 enter the lateral wall of the cavernous sinus, and V1 passes through the superior orbital fissure, while V2 passes through the foramen rotundum. V1 branches innervate the forehead, upper eyelid, and dorsum of the nose. V2 goes out of the foramen rotundum to the pterygopalatine fossa and innervates the upper lip, lower eyelid, front part of the temporal face, and upper part of the cheek. V3 emerges from the foramen ovale to the masticator space, runs between the lateral and medial pterygoid muscles, and enters to the mandibular canal. V3 innervates the chin, lower part of the cheek, and posterior part of the temporal region (Fig. 6).

Pathology

Perineural spread along the trigeminal nerves

PNS is a form of metastatic disease in which the tumor spreads along the endoneurium or perineurium of nerves. PNS of primary head and neck cancers commonly occurs along the branches of CN V and VII, causing trigeminal neuralgia [43]. PNS along V1 may be caused by lacrimal cancer, along V2 by nasal cavity, paranasal sinus, or hard plate cancer, and along V3 by oral cancer. If trigeminal neuralgia occurs after treatment, recurrence along these nerves should be assessed.

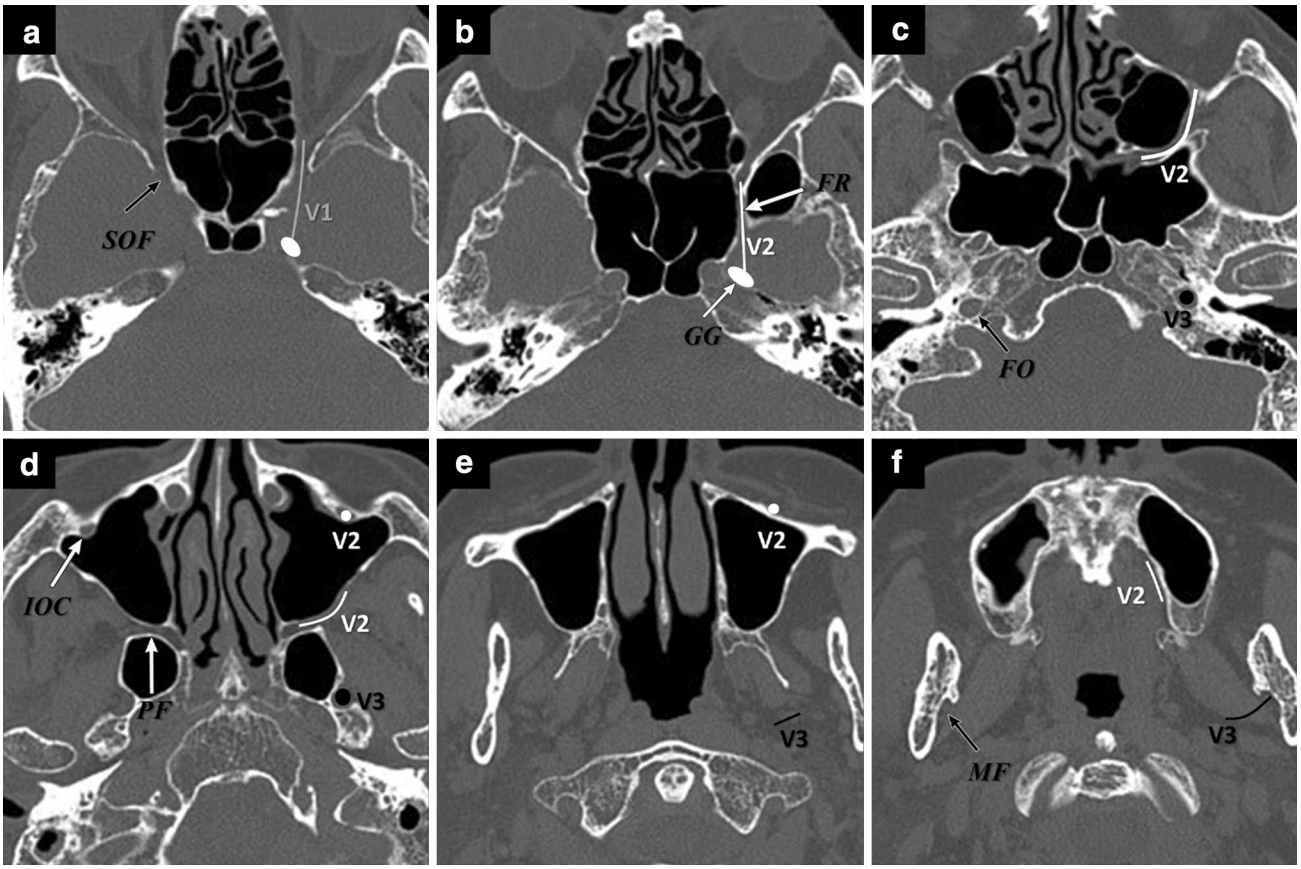

Fig. 6 Anatomy of the trigeminal nerve branches. The course of the V1 (gray), V2 (white), V3 (black) is shown. *SOF* superior orbital fissure, *FR* foramen rotundum, *GG* Gasserian ganglion, *FO* foramen ovale, *IOC* inferior orbital canal, *PF* pterygopalatine fossa, *MF* mandibular foramen

Imaging findings in PNS show foraminal enlargement or destruction, sclerotic changes around the foramina, obliteration of the fat planes, nerve enlargement or enhancement, neuropathic muscle atrophy, convexity of the lateral cavernous sinus wall, and replacement of the Meckel cave with soft tissue [43] (Fig. 7).

Numb chin syndrome

Numb chin syndrome is characterized by numbness in the region innervated by the mental nerve and is mainly caused by metastasis or hematopoietic tumors. Among patients with this syndrome at initial presentation, 27.7% have malignancy [44], the surveillance of which is essential for these patients. Thus, the V3 should be assessed in its entire length, from the mandible to the skull base (Fig. 8).

Otalgia

Associated anatomy and pathology

Otalgia is caused by an abnormality of the ear itself or involvement of the sensory (CN V, VII), glossopharyngeal (CN IX), vagus (CN X), and great auricular nerves. Otalgia perceived by stimulus of other sites such as oral cavity, pharynx or supraglottic larynx innervated by CN V3, IX, X, VII, C2, and C3 is called referred otalgia. Upper aerodigestive malignancy should be checked in cases of otalgia without ear abnormality [45] (Fig. 9).

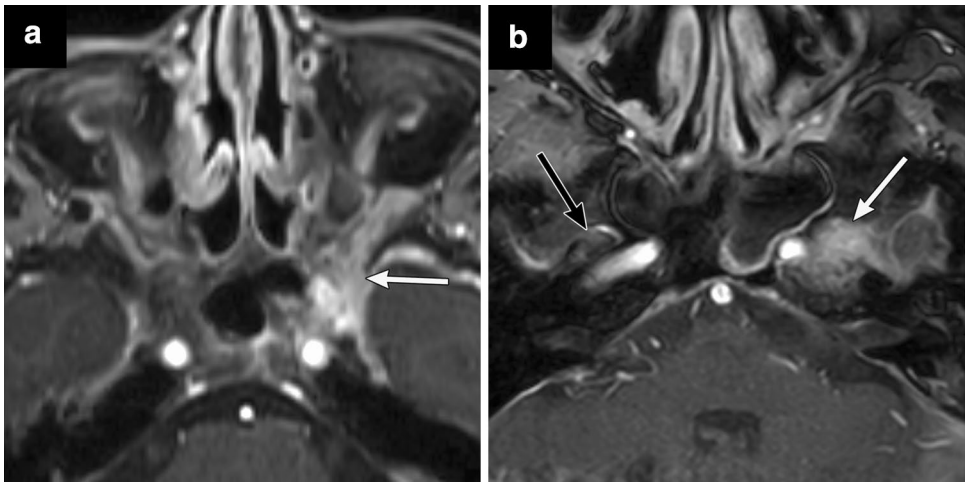

Fig. 7 A 77-year-old female with nasopharyngeal carcinoma and left facial numbness in V2 and V3 areas. **a** Post-contrast T1-weighted MR image showing perineural spread along the V2 extending to the cavernous sinus via the foramen rotundum (white arrow). **b** Post-contrast T1-weighted MR image showing perineural spread along the V3 extending to the foramen ovale (white arrow). The right foramen ovale is intact (black arrow)

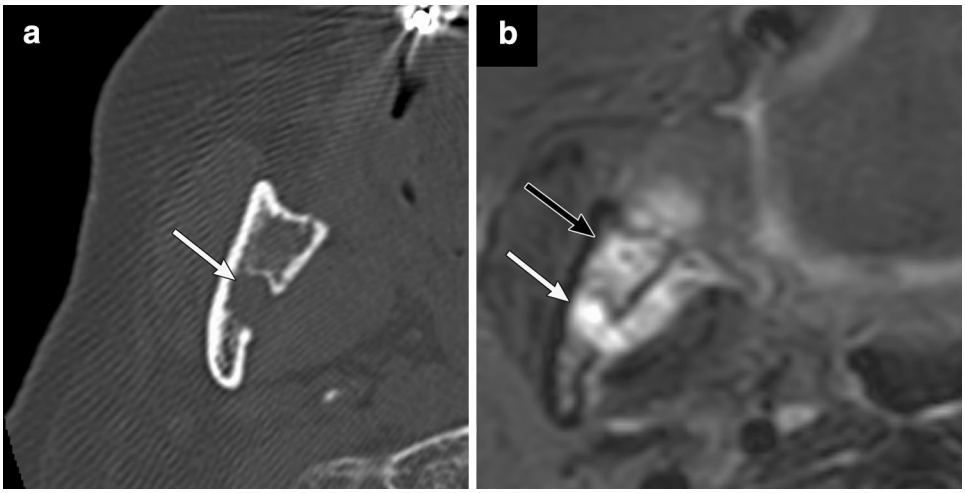

Fig. 8 A 76-year-old female with osteosarcoma and hypoesthesia at the submental area. **a** The mandibular foramen is widened on CT image (white arrow). **b** STIR (short tau inversion recovery) image showing the tumor invading the bone marrow (black arrow) and mandibular foramen (white arrow)

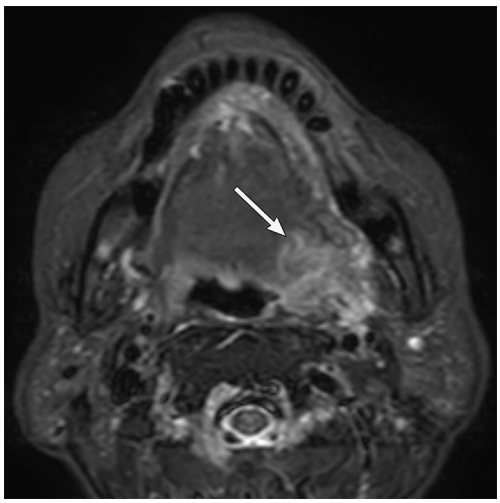

Fig. 9 A 68-year-old female with tongue cancer, post-operation. She had left otalgia at a routine follow-up. STIR (short tau inversion recovery) image shows local recurrence at the left tongue base (white arrow)

Dysgeusia

Associated anatomy and pathology

The anterior two-thirds of the tongue are innervated by the lingual and chorda nerves, responsible for sensation and taste, respectively, while the posterior third is innervated by CN IX, also responsible for sensation and taste. The lingual nerve is a branch of the V3. The chorda tympani branched from CN VII in the temporal bone, runs along the sphenopetrosal fissure, and then turns around the sphenoid spine, joining the lingual nerve. CN X carries taste from the back part of the mouth, including the upper third of the esophagus. Neoplasms invading the submandibular region or the skull base may cause dysgeusia [46] (Fig. 10).

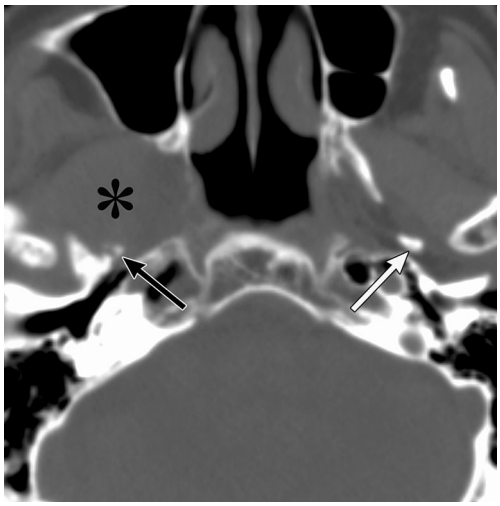

Fig. 10 A 60-year-old female with breast cancer and dysgeusia involving the right side of the tongue. Bone destruction of the right sphenoid spine (black arrow) due to a metastasis (asterisk) indicates tumor involvement of the chorda tympani on CT image. The normal left sphenoid spine (white arrow) is shown

Facial nerve paralysis

Associated anatomy

The path of the facial nerve can be divided into the labyrinth, tympanic, and mastoid segments in the extracranial part [47] (Fig. 11). The labyrinth segment starts from the fundus of the internal auditory canal to the first genu, where the greater superficial petrosal nerve and lesser petrosal nerves arise. In the tympanic segment, the facial nerve runs through the tympanic cavity, medial to the cochlea, while the mastoid segment starts from the second genu to the stylomastoid foramen. The facial nerve gives rise to the stapedius nerve and chorda tympani at the mastoid segment. Impairments in the greater superficial petrosal nerve, stapedius nerve, and chorda tympani cause disturbance in lacrimal secretion, hyperacusis, and dysgeusia with disturbance of salivary secretion, respectively. These symptoms are useful for predicting the location of facial nerve involvement.

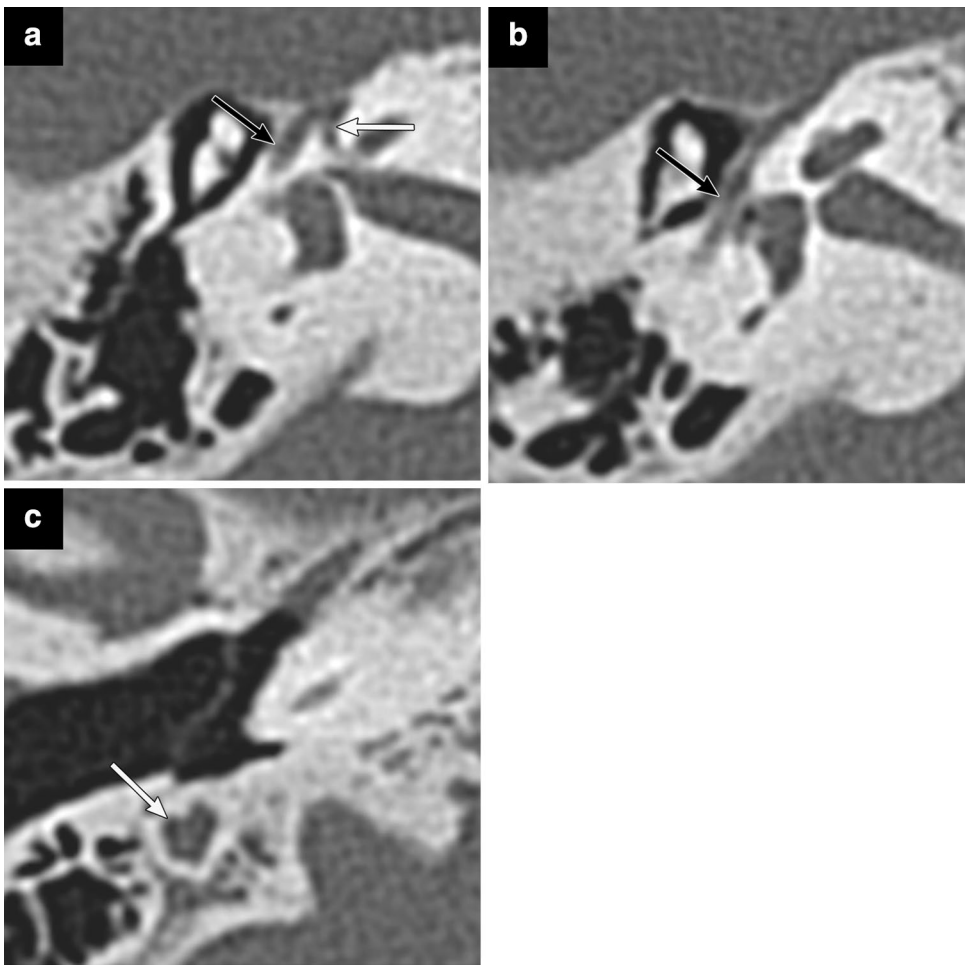

Fig. 11 Anatomy of the facial nerve. The labyrinth (white arrow in **a**) and the tympanic (black arrow in **a**, **b**) and mastoid (white arrow in **c**) segments are shown on high resolution CT images

Pathology

Direct invasion or perineural spread along CN VII

Parotid cancers may invade the facial nerve directly or by PNS (Fig. 12a, b). PNS in parotid cancers causes facial nerve paralysis, and their most common site is the mastoid segment of CN VII. PNS also appears along the peripheral side of the facial nerve and communicates with V3 via the auriculotemporal nerve or V2 via the greater superficial petrosal nerve [48]. CN VII supplies the motor branches to the stylohyoid muscle, the posterior belly of the digastric muscle, occipital muscle, and muscles of facial expression. Secondary degeneration of these muscles may be visible on imaging. Denervation initially causes edema and swelling of the muscle, evident as hyperintensities in T2-weighted MR images with contrast enhancement on T1-weighted MR images. In the chronic stage, imaging shows atrophy of the muscles with fat infiltration, associated decreased enhancement and T2-weighted hyperintensities [48]. If facial nerve paralysis occurs during the follow-up of parotid cancers, local recurrence as well as the facial nerve abnormalities within the temporal bone should be assessed.

Metastasis to the temporal bone

Temporal bone metastasis is seen at a late stage after the primary malignancy has already metastasized to other organs (Fig. 12c). Common primary malignancies include breast and lung cancer [49]. The most common otologic manifestations are facial palsy and hearing loss. The facial nerve is involved in 23% of the temporal bone metastasis cases [50], and the petrous apex is a common metastatic site due to its abundance in blood supply [49]. In contrast, metastasis to the inner ear is rare.

Dysphagia or dysarthria

Associated anatomy

Dysphagia or dysarthria may be caused by a disorder of the pharynx, larynx, oral cavity, or inferior CNs. CN IX and X

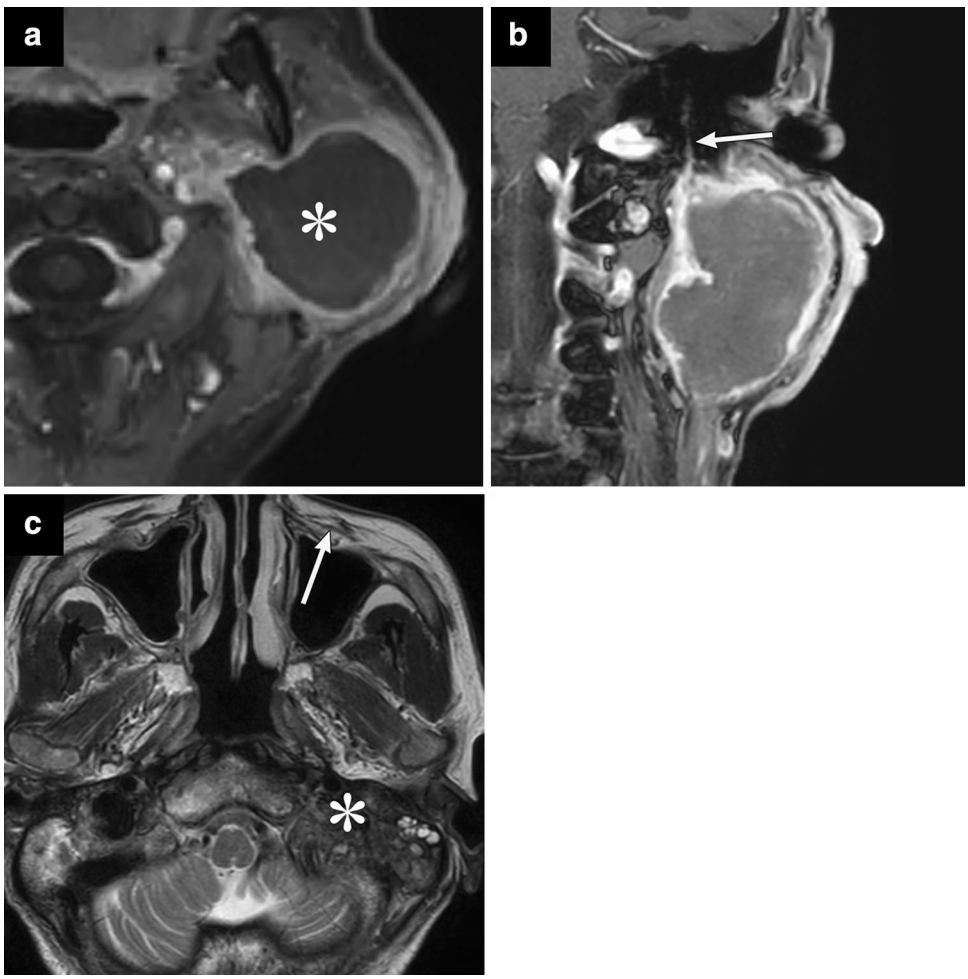

Fig. 12 **a**, **b** An 82-year-old man with a parotid cancer and left facial nerve paralysis. The parotid cancer (* in a, post-contrast T1-weighted MR image), replacing the left parotid gland, spreads along the left mastoid segment of the facial nerve (arrow in **b**, post-contrast coronal T1-weighted MR image). **c** A 63-year-old man with prostate cancer and left facial nerve paralysis. T2-weighted MR image shows metastasis (*) to the temporal bone involving the facial nerve of the mastoid segment. Secondary atrophy of the left zygomatic major muscle is also shown (white arrow)

emerge from the cranium via the jugular foramen and the hypoglossal nerve (CN XII) via the hypoglossal foramen and travel down along the carotid sheath (Fig. 13). CN IX bends anteriorly and courses between the stylopharyngeal and styloglossus muscles. The pharyngeal branch of CN X innervates most of the pharyngeal constrictor muscles. CN XII bends anteriorly and courses along the posterior belly of the digastric muscle, and enters the sublingual space. There, CN XII runs inferior to the lingual nerve. The landmark of CN IX is the stylopharyngeal and styloglossus muscles, while that of CN XII is the posterior belly of the digastric muscle, respectively [51].

Pathology

Perineural spread along the CN XII

Although less common, PNS caused by tongue-base or sublingual cancers may involve the hypoglossal nerve [52], which courses below along the posterior belly of the digastric muscle and loops over the hyoid bone. PNS of CN XII is showed as a tumor along this course of CN XII on imaging. Involvement of CN XII results in secondary degeneration of the tongue (Fig. 14a, b). Denervated muscles in the subacute phase show isointense to hypointense signals on T1-weighted MR images and hyperintense on T2-weighted MR images compared to normal muscle due to increased tissue water in the enlarged interstitial space. In the chronic stage, fat infiltration and atrophy of the affected side of the tongue are detected as increased T1 signal intensity [53]. Pseudohypertrophy, characterized by an increase in muscle volume due to fatty infiltration, may also be seen [54].

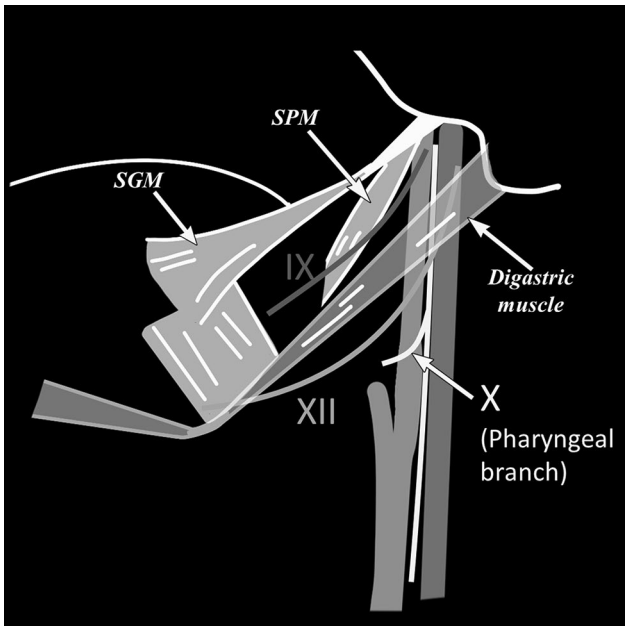

Fig. 13 A schema of the anatomy of CN IX, X and XII. The landmark of CN IX includes the stylopharyngeal muscle (SPM) and styloglossus muscle (SGM), while that of CN XII includes the posterior belly of the digastric muscle

Skull base osteomyelitis (SBO)

SBO is a serious infection of the skull base most frequently seen in elderly patients with diabetes but also in cancer patients after radiotherapy [55]. The condition is characterized by a subtle progression and nonspecific symptoms, such as otalgia and otorrhea, and is difficult to diagnose clinically. Differential diagnosis includes advanced nasopharyngeal carcinoma and skull base metastasis in cancer patients.

MRI findings in SBO include hypointensities of the bone marrow of the skull base on T1-weighted MR images, infiltration and obliteration of the parapharyngeal fat planes, and enhancement within the soft tissues adjacent to the skull base on T1-weighted MR images (Fig. 14c, d). The findings of hyperintensities on diffusion-weighted imaging and ring enhancement of the lesion, which represent an abscess, are helpful signs in SBO cases [56]. Abscesses tend to form in front of the clivus. The apparent diffusion coefficient value of SBO is lower than that of nasopharyngeal carcinoma, but there is no significant difference between SBO and metastatic lesions [57].

Skull base metastasis

Skull base metastasis may involve the jugular foramen and cause disorder of the inferior CNs. The jugular foramen syndrome consists of hoarseness, dysphagia, and unilateral dull and aching pain in the occipital and pharyngeal regions and is caused by involvement of the jugular foramen [58]. Most common primary cancer sites include the lung, breast, kidney, and gastrointestinal tract [59].

Hoarseness

Associated anatomy

Hoarseness is characterized by impairment of the vagus nerve and recurrent laryngeal nerve, in addition to abnormalities in the larynx itself. The vagus nerve runs through the jugular foramen, travels along the carotid sheath, and branches the upper laryngeal nerve at the lower cervical ganglion. The superior laryngeal nerve innervates the laryngopharyngeus and cricothyroid muscles. The recurrent laryngeal nerve loops under the aortic arch on the left and the brachiocephalic artery on the right, runs up the tracheoesophageal groove, and branches the inferior laryngeal nerve, which innervates other laryngeal muscles [60].

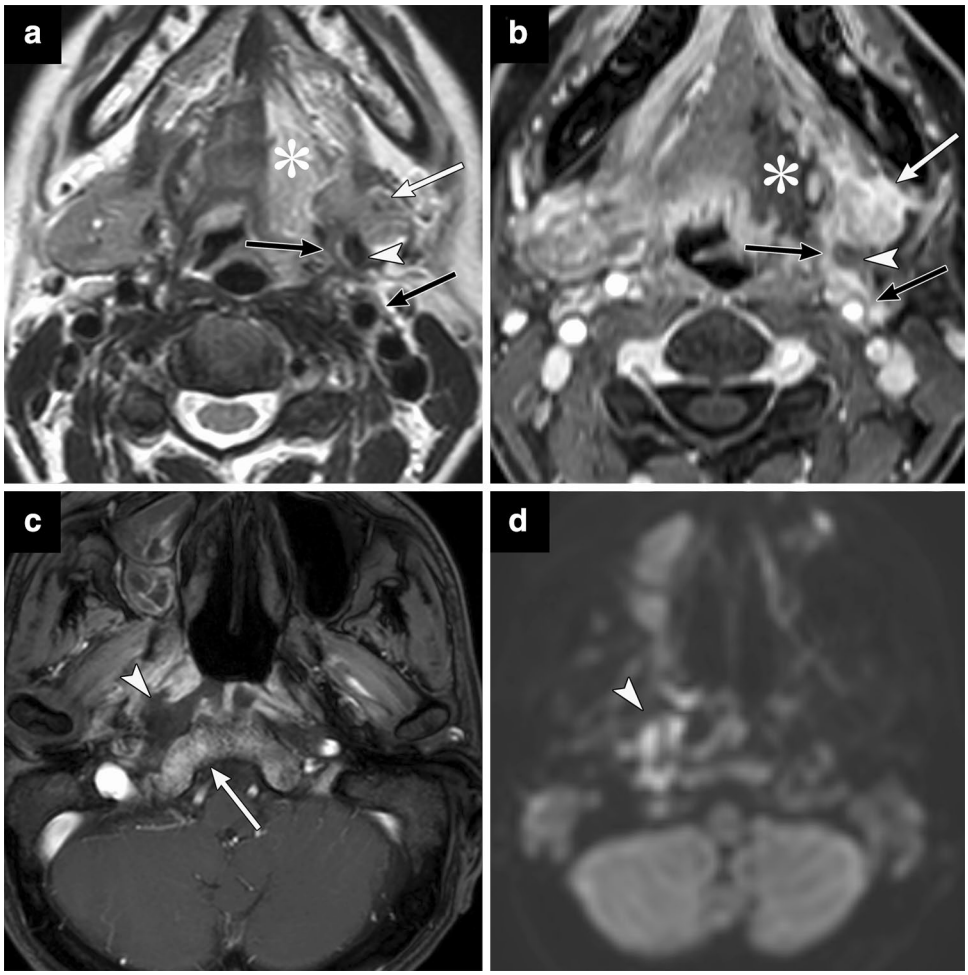

Fig. 14 Two cases with dysphasia. **a**, **b** A 51-year-old female with submandibular cancer. She had dysphagia and dysarthria. Perineural spread (black arrow in **a**: T2-weighted MR image, **b**: post-contrast T1-weighted MR image) continuing from the primary tumor (white arrow in **a**, **b**) extends lateral to the internal carotid artery and beneath the digastric muscle (arrowheads in **a**, **b**). This course is consistent with CN XII. The muscles of the left side of the tongue are denervated (* in **a**, **b**). **c**, **d** A 67-year-old male with nasopharyngeal carcinoma, after chemoradiation therapy. He had headache, dysphagia, and dysarthria. T1-weighted MR image shows enhancement of the clivus, indicating skull base osteomyelitis (white arrow in **c**). Lack of enhancement with hyperintensity on diffusion-weighted image in front of the clivus suggests abscess or necrotic tissue (arrowheads in **c**, **d**)

Pathology

Hoarseness is caused by lesions occurring at the upper mediastinum to the skull base. At the mediastinum, lung cancer or subaortic lymph node metastasis may involve recurrent laryngeal nerve. At the lower neck, thyroid cancer or nodal metastasis with extranodal extension invades the laryngeal recurrent nerves running at the tracheoesophageal groove. Laryngeal or hypopharyngeal cancer may invade the glottis directly. At the skull base, bone metastasis may involve the jugular foramen. Iatrogenic injury of the recurrent laryngeal or vagus nerves during procedures in the neck, chest, and skull base, such as thyroid and parathyroid surgery, as well as complications during endotracheal intubation, may also cause hoarseness [61].

On imaging, the signs of vocal cord paralysis include atrophy of the affected vocal cord muscle, ipsilateral piriform sinus dilatation, ipsilateral laryngeal ventricle dilatation, and medial rotation and thickening of the aryepiglottic fold [62, 63] (Fig. 15). Other signs include the anteromedial displacement of the ipsilateral arytenoid cartilage and medial displacement of the posterior vocal cord margin. These findings result in the residual airway having a shape similar to a ship's sail, which is commonly referred to as the "sail" sign [60].

Syncope

Associated anatomy

Syncope is classified into three categories: reflex/neural-mediated, orthostatic hypotension-mediated, and cardiac syncope. Reflex-mediated syncope comprises vasovagal and situational syncope, carotid sinus syndrome, and glossopharyngeal neuralgia. The most common reflex cardiovascular syndromes linked to CN IX are the carotid sinus and glossopharyngeal neuralgia-asystole syndromes. These cause the reflex cardiovascular syncope, in which the glossopharyngeal nerve constitutes the afferent nerve pathway. Afferent fibers of the glossopharyngeal nerve project to the solitary tract nucleus, from which efferent fibers descend into the vagus [64].

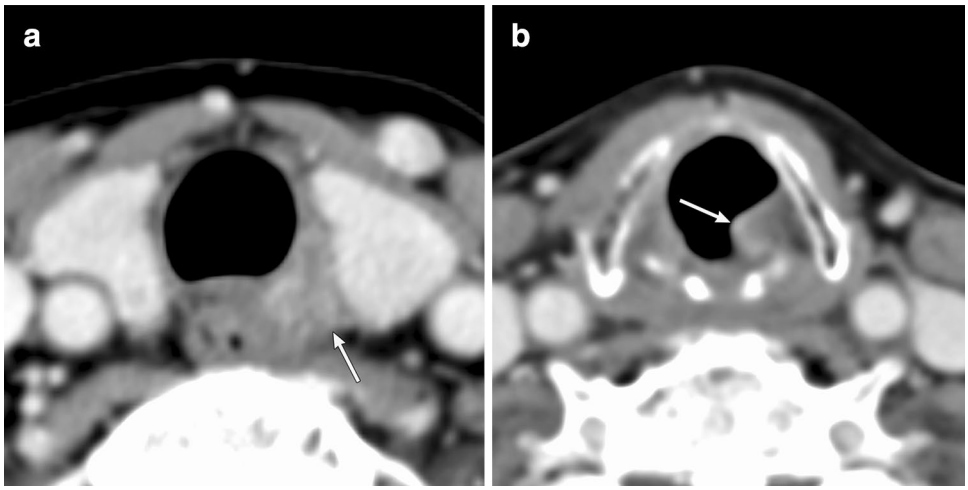

Fig. 15 A 54-year-old female with thyroid cancer and hoarseness. **a** Contrast-enhanced CT image showing the thyroid cancer invading the left tracheoesophageal groove (white arrow). **b** Medial displacement of the posterior margin of the left vocal cord suggests left vocal cord paralysis (white arrow)

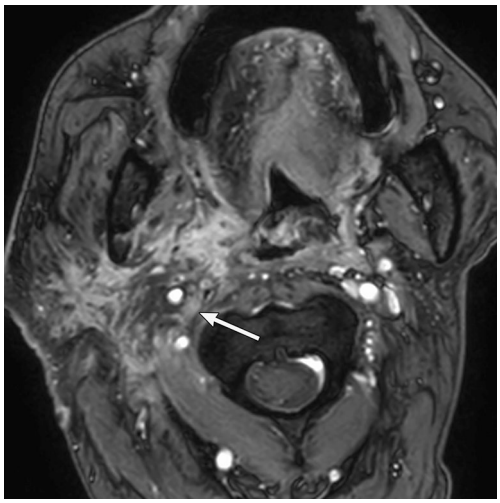

Fig. 16 A 65-year-old man with recurrence of oral cancer and repeated syncope. Post-contrast T1-weighted MR image shows the recurrent tumor invades around the right carotid sheath. Repeated syncope is caused by the vagal reflex due to tumor invasion to the carotid sheath (white arrow)

Pathology

Reflex-mediated syncope is caused by mechanical traction or invasion of the carotid sinus by a tumor or lymph node metastasis, or by stimulation of CN IX by the tumor. Reflex syncope associated with malignancy is rare, and its prevalence was estimated at 0.4% in a series of 4500 patients with head and neck cancer [65]. Head and neck cancer is the most frequent malignancy causing reflex syncope. However, lymphomas, neurofibromas, metastatic breast, and esophageal or lung malignancies have also been reported [64]. On imaging, the lesion infiltrates the carotid sheath or bifurcation (Fig. 16).

Syndromes associated with multiple CN involvement

The extension of the skull base involvement is possible to estimate from a combination of neurological symptoms. Various syndromes associated with CNs have been reported (Table 2) [24, 25, 32–34, 58, 59, 66, 67]. The superior

Table 2 Summary of syndromes associated with multiple cranial nerve involvement

Syndrome	Nerves	Locations
Superior orbital fissure syndrome	III, IV, V1, VI	Superior orbital fissure
Orbital apex syndrome	II, III, IV, V1, VI	Optic canal Superior orbital fissure
Cavernous sinus syndrome	III, IV, V1, V2, VI	Cavernous sinus
Gradenigo/pseudo-Gradenigo syndrome	V, VI	Petrous apex
Vernet (jugular foramen) syndrome	IX, X, XI	Jugular foramen
Collet–Sicard syndrome	IX, X, XI, XII	Jugular foramen Hypoglossal canal
Villaret syndrome	IX, X, XI, XII, sympathetic nerves	Jugular foramen Hypoglossal canal Carotid canal

II optic nerve, *III* oculomotor nerve, *IV* trochlear nerve, *V* trigeminal nerve, *VI* abducens nerve, *IX* glossopharyngeal nerve, *X* vagus nerve, *XI* accessory nerve, *XII* hypoglossal nerve

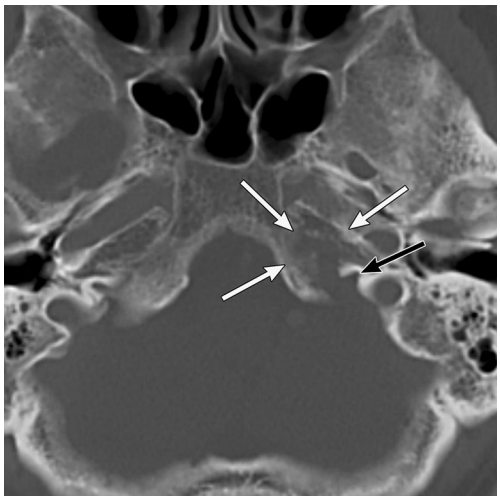

Fig. 17 A 73-year-old man with cholangiocarcinoma and paralysis of the left CN IX–XI (jugular foramen syndrome). Lesion of the left jugular foramen is clinically suspected. CT image shows occipital bone metastasis (white arrows) involving the left par nervosa of the jugular foramen (black arrow)

orbital fissure, orbital apex, cavernous sinus, Gradenigo, pseudo-Gradenigo, and jugular foramen syndromes (Vernet syndrome, Fig. 17) were mentioned earlier in the present article. Besides these syndromes, syndromes involving the inferior CNs include the Collet–Sicard syndrome characterized by impairments in CN IX–XII and the retroparotid space syndrome (Villaret syndrome) characterized by impairments in CN IX–XII and sympathetic nerve [66, 67]. These syndromes may be caused by head and neck cancer including parotid cancer and nasopharyngeal carcinoma, skull base osteomyelitis, and skull base metastasis.

Conclusions

Neurological symptoms associated with head and neck lesions are induced in a complicated manner by complex anatomy and various causes. A thorough understanding of the extracranial neuroanatomy and pathology helps in identifying lesions on CT/MR imaging. Thus, a symptom-based imaging approach can ensure optimal therapeutic outcome in cancer patients.

Acknowledgements This article was supported by Canon Medical systems.

Funding This article was supported by Canon Medical systems.

Compliance with ethical standards

Conflict of interest Tatsushi Kobayashi and Masahiko Kusumoto have funding from Canon Medical Systems. Masahiko Kusumoto has honoraria or fees for promotional materials from Ono pharmaceutical co., Ltd, Astra Zeneca K.K. and MSD K.K. The other authors declare that they have no conflict of interest.

Ethical statement This manuscript is a review article and has no studies with human participants or animals performed by any of the authors.

References

1. Cancer Registry and Statistics. Cancer information service. Tokyo: National Cancer Center; 2014.
2. Teunissen SCCM, Wesker W, Kruitwagen C, de Haes HCJM, Voest EE, de Graeff A. Symptom prevalence in patients with incurable cancer: a systematic review. J Pain Symptom Manag. 2007;34:94–104.
3. Clouston PD, DeAngelis LM, Posner JB. The spectrum of neurological disease in patients with systemic cancer. Ann Neurol. 1992;31:268–73.
4. Gilbert MR, Grossman SA. Incidence and nature of neurologic problems in patients with solid tumors. Am J Med. 1986;81:951–4.
5. Hallinan JTPD, Pillay P, Koh LHL, Goh KY, Yu WY. Eye globe abnormalities on MR and CT in adults: an anatomical approach. Korean J Radiol. 2016;17:664–73.
6. Ferry AP, Font RL. Carcinoma metastatic to the eye and orbit. I. A clinicopathologic study of 227 cases. Arch Ophthalmol. 1974;92:276–86.
7. Shields CL, Shields JA, Gross NE, Schwartz GP, Lally SE. Survey of 520 eyes with uveal metastases. Ophthalmology. 1997;104:1265–76.
8. Miyabo H, Mori H, Tokunag N. Outcome of vitreous surgery in a case of total detachment due to choroidal metastasis from breast carcinoma. Jpn J Clin Ophthalmol. 2017;71:761–5.
9. Lemke AJ, Hosten N, Wiegel T, Prinz RD, Richter M, Bechrakis NE, et al. Intraocular metastases: differential diagnosis from uveal melanomas with high-resolution MRI using a surface coil. Eur Radiol. 2001;11:2593–601.
10. Jorg D, Vinai G, Minesh M. Delayed complications of cranial irradiation. UpToDate. 2018. https://www.uptodate.com/contents/delayed-complications-of-cranial-irradiation.
11. Mayo C, Martel MK, Marks LB, Flickinger J, Nam J, Kirkpatrick J. Radiation dose-volume effects of optic nerves and chiasm. Int J Radiat Oncol Biol Phys. 2010;76:S28–35.
12. Danesh-Meyer HV. Radiation-induced optic neuropathy. J Clin Neurosci. 2008;15:95–100.
13. McClellan RL, el Gammal T, Kline LB. Early bilateral radiation-induced optic neuropathy with follow-up MRI. Neuroradiology. 1995;37:131–3.
14. Cherekaev VA, Lasunin NV, Stepanian MA, Rotin DL, Grigor'eva NN, Vetlova ER, et al. Breast carcinoma metastasis to the optic nerve: case report and review of literature. Zh Vopr Neirokhir Im N N Burdenko. 2013;77:42–8.
15. Tailor TD, Gupta D, Dalley RW, Keene CD, Anzai Y. Orbital neoplasms in adults: clinical, radiologic, and pathologic review. Radiographics. 2013;33:1739–58.
16. Albert DM, Rubenstein RA, Scheie HG. Tumor metastasis to the eye. II. Clinical study in infants and children. Am J Ophthalmol. 1967;63:727–32.
17. Pojskic M, Zbytek B, Arnautovic KI. Anterior clinoid metastasis removed extradurally: first case report. J Neurol Surg Rep. 2018;79:e55–62.

18. Thust SC, Yousry T. Imaging of skull base tumours. Reports Rep Pract Oncol Radiother. 2016;21:304–18.
19. Chen L, Jiang L, Yang B, Subramanian PS. Clinical features of visual disturbances secondary to isolated sphenoid sinus inflammatory diseases. BMC Ophthalmol. 2017;17:237.
20. Zubizarreta PA, D'Antonio G, Raslawski E, Gallo G, Preciado MV, Casak SJ, et al. Nasopharyngeal carcinoma in childhood and adolescence: a single-institution experience with combined therapy. Cancer. 2000;89:690–5.
21. Gray ST, Sadow PM, Lin DT, Sedaghat AR. Endoscopic sinus surgery for chronic rhinosinusitis in patients previously treated for sinonasal malignancy. Laryngoscope. 2016;126:304–15.
22. Van Tassel P, Lee YY, Jing BS, De Pena CA. Mucoceles of the paranasal sinuses: MR imaging with CT correlation. AJR Am J Roentgenol. 1989;153:407–12.
23. Yagi A, Sato N, Taketomi A, Nakajima T, Morita H, Koyama Y, et al. Normal cranial nerves in the cavernous sinuses: contrast-enhanced three-dimensional constructive interference in the steady state MR imaging. AJNR Am J Neuroradiol. 2005;26:946–50.
24. Yoshida K, Shirata A, Sato T, Kishida Y, Saito K, Yamane K. A case of orbital apex syndrome due to aspergillus infection that avoided loss of visual acuity by optic canal decompression. Rinsho Shinkeigaku. 2016;56:1–6.
25. Evans HH, Wurth BA, Penna KJ. Superior orbital fissure syndrome: a case report. Craniomaxillofac Trauma Reconstr. 2012;5:115–20.
26. Remington LA. Chapter 11—Orbital blood supply. In: Lee AR, Denise G, editors. Clinical anatomy of the visual system. 2nd ed. Oxford: Butterworth-Heinemann; 2012. p. 202–17.
27. Piffer CR, Zorzetto NL. Course and relations of the abducens nerve. Anat Anz. 1980;147:42–6.
28. Arnold RW, Adams BA, Camoriano JK, Dyer JA. Acquired divergent strabismus: presumed metastatic gastric carcinoma to the medial rectus muscle. J Pediatr Ophthalmol Strabismus. 1989;26:50–1.
29. Leung V, Wei M, Roberts TV. Metastasis to the extraocular muscles: a case report, literature review and pooled data analysis. Clin Exp Ophthalmol. 2018;46:687–94.
30. Capone AJ, Slamovits TL. Discrete metastasis of solid tumors to extraocular muscles. Arch Ophthalmol. 1990;108:237–43.
31. Homer N, Jakobiec FA, Stagner A, Cunnane ME, Freitag SK, Fay A, et al. Periocular breast carcinoma metastases: correlation of clinical, radiologic and histopathologic features. Clin Exp Ophthalmol. 2017;45:606–12.
32. van Overbeeke JJ, Jansen JJ, Tulleken CA. The cavernous sinus syndrome. An anatomical and clinical study. Clin Neurol Neurosurg. 1988;90:311–9.
33. Tornabene S, Vilke GM. Gradenigo's syndrome. J Emerg Med. 2010;38:449–51.
34. Azarmina M, Azarmina H. The six syndromes of the sixth cranial nerve. J Ophthalmic Vis Res. 2013;8:160–71.
35. Lee JH, Lee HK, Lee DH, Choi CG, Kim SJ, Suh DC. Neuroimaging strategies for three types of Horner syndrome with emphasis on anatomic location. AJR Am J Roentgenol. 2007;188:W74–81.
36. Mansour AM, Hidayat AA. Metastatic eyelid disease. Ophthalmology. 1987;94:667–70.
37. Martorell-Calatayud A, Requena C, Díaz-Recuero JL, Haro R, Sarasa JL, Sanmartín O, et al. Mask-like metastasis: report of 2 cases of 4 eyelid metastases and review of the literature. Am J Dermatopathol. 2010;32:9–14.
38. Davagnanam I, Fraser CL, Miszkiel K, Daniel CS, Plant GT. Adult Horner's syndrome: a combined clinical, pharmacological, and imaging algorithm. Eye. 2013;27:291–8.
39. Pruitt JA, Ilsen PF. On the frontline: what an optometrist needs to know about myasthenia gravis. Optometry. 2010;81:454–60.
40. Li W, Miao Z, Liu X, Zhang Q, Sun L, Li P, et al. Thymic carcinoma patients with myasthenia gravis exhibit better prognoses. Int J Clin Oncol. 2016;21:75–80.
41. Hülsbrink R, Hashemolhosseini S. Lambert–Eaton myasthenic syndrome—diagnosis, pathogenesis and therapy. Clin Neurophysiol. 2014;125:2328–36.
42. Kamel HAM, Toland J. Trigeminal nerve anatomy. Am J Roentgenol. 2001;176:247–51.
43. Caldemeyer KS, Mathews VP, Righi PD, Smith RR. Imaging features and clinical significance of perineural spread or extension of head and neck tumors. RadioGraphics. 1998;18:97–110.
44. Galan SG, Penarrocha MD, Penarrocha DM. Malignant mental nerve neuropathy: systematic review. Med Oral Patol Oral Cir Bucal. 2008;13:E616–21.
45. Charlett SD, Coatesworth AP. Referred otalgia: a structured approach to diagnosis and treatment. Int J Clin Pract. 2007;61:1015–21.
46. Heckmann JG, Heckmann SM, Lang CJG, Hummel T. Neurological aspects of taste disorders. Arch Neurol. 2003;60:667–71.
47. Ho M-L, Juliano A, Eisenberg RL, Moonis G. Anatomy and pathology of the facial nerve. AJR Am J Roentgenol. 2015;204:W612–9.
48. Gandhi M, Sommerville J. The imaging of large nerve perineural spread. J Neurol Surg B Skull Base. 2016;77:113–23.
49. Gloria-Cruz TI, Schachern PA, Paparella MM, Adams GL, Fulton SE. Metastases to temporal bones from primary nonsystemic malignant neoplasms. Arch Otolaryngol Head Neck Surg. 2000;126:209–14.
50. Song K, Park K-W, Heo J-H, Song I-C, Park Y-H, Choi JW. Clinical characteristics of temporal bone metastases. Clin Exp Otorhinolaryngol. 2019;12:27–32.
51. Sekiya K. Perineural spread. In: Kaneda T, Kuno H, editors. A key to jaw, teeth, oral cavity imaging. Tokyo: Gakken Medical Shujunsha; 2017. p. 184–5.
52. Paes FM, Singer AD, Checkver AN, Palmquist RA, De La Vega G, Sidani C. Perineural spread in head and neck malignancies: clinical significance and evaluation with 18F-FDG PET/CT. Radiographics. 2013;33:1717–36.
53. Murakami R, Baba Y, Nishimura R, Furusawa M, Baba T, Okuda T, et al. CT and MR findings of denervated tongue after radical neck dissection. AJNR Am J Neuroradiol. 1997;18:747–50.
54. Russo CP, Smoker WR, Weissman JL. MR appearance of trigeminal and hypoglossal motor denervation. AJNR Am J Neuroradiol. 1997;18:1375–83.
55. Lalani N, Huang SH, Rotstein C, Yu E, Irish J, O'Sullivan B. Skull base or cervical vertebral osteomyelitis following chemoradiotherapy for pharyngeal carcinoma: a serious but treatable complication. Clin Transl Radiat Oncol. 2018;8:40–4.
56. Parmar HA, Sitoh Y-Y. Diffusion-weighted imaging findings in central skull base osteomyelitis with pharyngeal abscess formation. AJR Am J Roentgenol. 2005;184:1363–4.
57. Ozgen B, Oguz KK, Cila A. Diffusion MR imaging features of skull base osteomyelitis compared with skull base malignancy. Am J Neuroradiol. 2011;32:179–84.
58. Laigle-Donadey F, Taillibert S, Martin-Duverneuil N, Hildebrand J, Delattre J-Y. Skull-base metastases. J Neurooncol. 2005;75:63–9.
59. Caldemeyer KS, Mathews VP, Azzarelli B, Smith RR. The jugular foramen: a review of anatomy, masses, and imaging characteristics. Radiographics. 1997;17:1123–39.
60. Paquette CM, Manos DC, Psooy BJ. Unilateral vocal cord paralysis: a review of CT findings, mediastinal causes, and the course of the recurrent laryngeal nerves. Radiographics. 2012;32:721–40.
61. Reiß M, Reiß G. Hoarseness—causes and treatments. Med Monatsschr Pharm. 2016;39:429–35.

62. Agha FP. Recurrent laryngeal nerve paralysis: a laryngographic and computed tomographic study. Radiology. 1983;148:149–55.
63. Kumar VA, Lewin JS, Ginsberg LE. CT assessment of vocal cord medialization. AJNR Am J Neuroradiol. 2006;27:1643–6.
64. Casini A, Tschanz E, Dietrich PY, Nendaz M. Recurrent syncope due to esophageal squamous cell carcinoma. Case Rep Oncol. 2011;4:433–8.
65. Macdonald DR, Strong E, Nielsen S, Posner JB. Syncope from head and neck cancer. J Neurooncol. 1983;1:257–67.
66. Villatoro R, Romero C, Rueda A. Collet-Sicard syndrome as an initial presentation of prostate cancer: a case report. J Med Case Rep. 2011;5:315.
67. Flis DW, Shah AT, Tracy JC, Heilman CB, O'Leary MA. Metastatic breast carcinoma of the jugular foramen: a rare case of Villaret syndrome. Head Neck. 2015;37:E146–9.